5-1-1984

Photometric processing and interpretation of ratioed imagery by multivariate discriminant analysis for separation of geological types

Donald Marsh

PHOTOMETRIC PROCESSING AND INTERPRETATION OF RATIOED IMAGERY BY MULTIVARIATE DISCRIMINANT ANALYSIS FOR SEPARATION OF GEOLOGICAL TYPES

Donald Jay Marsh

April, 1984

PHOTOMETRIC PROCESSING AND INTERPRETATION OF RATIOED IMAGERY BY MULTIVARIATE DISCRIMINANT ANALYSIS FOR SEPARATION OF GEOLOGICAL TYPES

by

Donald Jay Marsh

A thesis submitted in partial fulfillment
of the requirements for the degree of
Bachelor of Science in the School of
Photographic Arts and Sciences in the
College of Graphic Arts and Photography
of the Rochester Institute of Technology

Signature of the Author .....
Imaging and Photographic
Science

Certified by .....
Thesis Advisor

Accepted by .....
Supervisor, Undergraduate Program

THESIS RELEASE PERMISSION FORM

ROCHESTER INSTITUTE OF TECHNOLOGY

COLLEGE OF GRAPHIC ARTS AND PHOTOGRAPHY

Title of Thesis: Photometric Processing and Interpretation of Ratioed Imagery by Multivariate Discriminant Analysis for Separation of Geological Types.

I, Donald Jay Marsh, hereby grant permission to Wallace Memorial Library, of R.I.T. to reproduce my thesis in whole or in part. Any reproduction will not be for commercial use of profit.

Date: 3/14/84

PHOTOMETRIC PROCESSING AND INTERPRETATION OF RATIOED IMAGERY BY MULIVARIATE DISCRIMINANT ANALYSIS FOR SEPARATION OF GEOLOGICAL TYPES

by

Donald Jay Marsh

Submitted to the Imaging and Photographic Science Division in partial fulfillment of the requirements for the Bachelor of Science degree at the Rochester Institute of Technology

ASTRACT

A study has investigated the ability of ratioed information from Landsat 2 Multispectral imagery, to discriminate geological features through the application of photometric processing techniques. United States Geological survey maps corresponding to the areas investigated have been used in correlation with ratioed imagery to identify predict and confirm geological features on the basis of resulting densitometric information. A multivariate, discriminant analysis of rock type, exposure data has enabled the fabrication of the final, optimized ratio image. The optimization process used to predict geological types involved a priority structure that found the spectral bands with the highest discriminatory power and the least correlation and

then predicted contrast values for the positive and negative masks. Lab test imagery of several rock samples provided imputus for further investigation from the chosen orbital imaging system, the Landsat Satellite series.

ACKNOWLEDGEMENTS

Completion of this project was made possible by the technical assistance and support of many persons:

Dr. John Schott for his technical support and assistance in getting the project off the ground and continually providing new ideas.

The R.I.T., Rochester and National branch of the Society of Photographic Scientists and Engineers for their many conferences in which numerious ideas have given the author deep insight into new and inovative concepts.

The Imaging Science Faculty at R.I.T., my family and friends for their mental and physical support, notably my father, who time and time again kept me striving for my personal best.

DEDICATION

The author would like to dedicate this work to the memory of John Cobb. The life of Mr. Cobb has made a profound impact on the aspirations and accomplishments of the author. With his death, a world of possibilities and personal dreams that seemed impossible, became reality. It is to his living memory that I present this work.

TABLE OF CONTENTS

LIST OF TABLES

RESULTS SECTION

LIST OF FIGURES

Introduction

Progress in Remote Sensing since the early 1950's has utilized multiple data acquisition and analysis techniques. [1] The so-called "multi" concept used in remote sensing has several advantages and limitations which are a function of the intended use of the resultant information. Imagery of the earth, used for the collection of Environmental Resource Data has taken these problems and assets into account.

Remote Sensing is concerned with the recording of electromagnetic radiation onto an imaging system. Sensing of the earth from above the ground can be accomplished by some imaging systems that view features in different parts of the spectrum simultaneously. This has been refered to as multispectral or multiband imaging. Given a specific composition of a ground feature, the energy reflecting from that element is a function of many molecular characteristics of the feature. The spectral reflectance of the body results in its own unique spectral signature and is in some way a function of the signal produced by the electromagnetic sensor. Multispectral photography uses this natural phenomenon to its advantage and records information separately so the spectral signatures can be identified from one another. Manifested differences in the spectral reflectance between features appear as signal differences on the ensuing image and can be

used to differentiate those features.

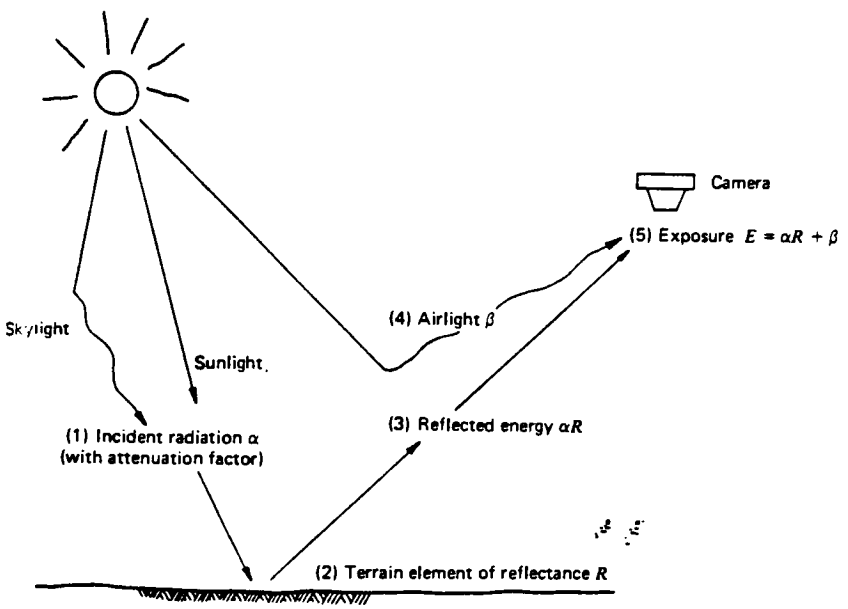

Figure 1. Factors Relating Film Exposure to Ground Reflectance.

Much recent information has been dedicated to digital imagery because of the speed of calculation, analysis and evaluation. A many-fold increase in efficiency of handling large amounts of data has been realized. The discipline of multispectral image analysis has seen the capability of data transformation take a quantum leap since the early nineteen sixties. Simple transformations such as the ratio of picture elements (pixels) from two images is quite commonplace. Numerical pixel data is highly informative and produces high quality results with a minimum of loss in the system. Limitations imposed by the digital process include space, time, expensive equipment and high cost. It is possible

however to emulate the superior "digital process" through photographic processes. Work related to this field has developed before computers became increasingly efficient and substantial techniques have been developed to separate and extract spectral reflectivity variations and other optical and ground-atmosphere interaction effects [2].

Ratioed images can be used to enhance the discrimination of ground features as well as making quantitative analysis of the spectral reflectance of the feature. Digital ratioed images are generated by dividing pixel values in one multispectral band by the corresponding values in another band. Photographic ratio images are made by superimposing negative and positive contrast images of two spectral regions.

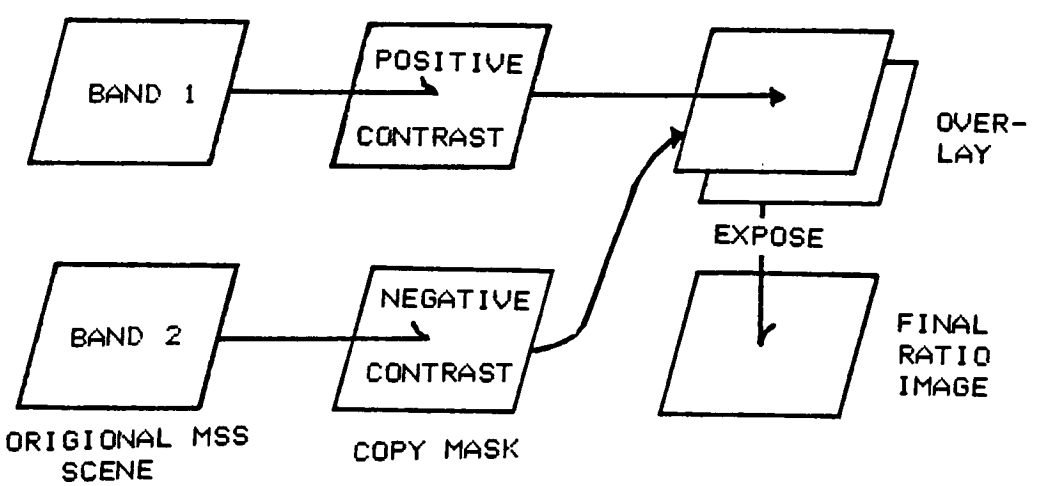

Figure 2. Photographic Ratio Mask Production.

In a matrix (x,y), the ratio of the signals of the two bands

i and j can be written;

$$r(i,j) = \frac{S(x,y,\ i)}{S(x,y,\ j)} \qquad \text{(eqn 1)}$$

The ability of ratioed images to negate various extranious multiplicative factors that effect photographic radiometric data as well as sensor data has been established by many authors in recient years [3]. Spectral ratios negate mulitplicative factors within the sensor data that act equally in all wavelengths of analysis. Differential illumination caused by changes in the atmosphere or topographical effects across a scene are negated. In addition, multispectral ratios provide a good estimate of the average scene brightness and eliminates confusion between reflected electromagnetic radiation and other variations. Topographically induced brightness variations of individual spectral bands has been a problem that has limited the success of many studies of reflected radiation since the early 1960's [4]. It is assumed that the modulation of the brightness of a scene due to topography is generally independent of material properties and wavelength spectra, therefore multispectral band ratios can be used to discriminate material properties. Ratioing eliminates relief shading and it has been suggested that the stereoscopic effect could be used to enhance the three dimensional context of spectral patterns so as to more fully see the three dimensional representation of the spectral components [5,6].

In theory each type of ground feature has a specific spectral signature which can be identified using appropriate spectral sensing equipment. In reality spectral reflectance curves of any given feature are affected by many things contributing to the degradation and blurring of the final product. These signatures may even vary within a certain species, from one site to another. A few factors influencing soil reflectance, are moisture content, soil texture, (proportion of sand and clay) surface roughness, the presence of iron oxide, and organic matter content. It is thought that the separation of geological types will also have these types of errors. It has been shown that soil moisture and texture patterns as well as surface roughness play an important part in the quantitative analysis of the spectral characteristics within a land form element [7]. Increased moisture content of a given soil and increased texture or size of the soil particles will give a lower exposure to the sensing system. Correspondence of these theories in investigations of rock types is expected and will be treated in final evaluations.

Many factors influence the sensing of ground features from the air as both spatial and spectral resolution of the recording are affected. Atmospheric effects and ground interactions encompass many of the problems associated with remote sensing. The key to geologic identification systems by remote sensing means relies on identification of relationships

between reflectance values of the ground feature and its resulting exposure. Exposure at a given point also depends on meterological conditions, altitude of measurement and illumination (sun and thermal infared self-emmision) conditions [8].

Directly reflected sunlight as well as skylight and airlight (the amount of illumination scattered by the air below the imaging system) contribute to the exposure. Atmospheric factors can be expressed mathematically and ground reflectances may be related to exposure by the following equation.

$$E = \sigma R + \beta \quad \text{or} \quad R = \frac{E - \beta}{\sigma} \quad \text{(eqn 2)}$$

where:

E = Total energy (exposure)on the film at a given point.
σ = A factor proportional to sunlight and skylight on the ground feature, reduced to include the effect of atmospheric attenuation.
R = Reflectance of the ground feature.
β = Airlight: additional energy received by the imaging system from the atmosphere and not from the object. [9 & 10]

As the amount of electromagnetic energy reaching the imaging system changes, the transmittance of the image and density can be translated to exposure values via the characteristic curve for conversion back to reflectance of the object. Methods have been proposed for estimating (σ) and (β) by using calibrated reflectance panels positioned on the

ground or a Scene Color Standard (SCS) Technique [11]. The SCS technique uses exposure measurements of density from inside and outside shadowed areas of uniform reflectance. Radiative transfer methods have been proposed to quantify atmospheric attenuation between the ground and the imaging platform to obtain a better value of σ. Atmospheric attenuation and haze are the principle components owing to the nontemporal degredation of remotely sensed data. Quantification of their parameters allows better calculation of the exposure and the ensuing signal from the ground element of reflectance R. The two major methods used to solve for σ and β are the Shadow [12] and Reflection Technique [13].

Atmospheric effects include scattering and absorption of energy. Scattering occurs when electromagnetic radiation is relflected or refracted by particles in the atmosphere. Radiation can also be absorbed by the atmosphere in differing amounts at different wavelength. Rayliegh scattering occurs when the radation wavelength is much larger than the size of the scattering particles. Mie scattering occurs where the particle size is comparable to the radiation wavelength. Water vapor and aerosols in the atmospnere contribute to the attenuation of incident wavefronts reaching ground features. The value of α gives a coefficient which is proportional to this attenuation. Nonselective scattering occurs when the particle size is much larger than the wavelength of interest.

Water droplets and ice crystals are examples of this type of scatter. Absorption, reflection and refraction occur across the spectrum. The molecular structures and hence the photometric properties of the constituent molecules in the atmosphere contribute to the nonselective scattering. Physical measurement of the quantities involved found by atmospheric measuring instruments in the calculations of scatter have been obtained. Simple addition of wavelength dependant coefficients will produce transmission versus wavelength data for the entire electromagnetic spectrum. Figure 3 gives average spectral transmittance of the atmosphere and average spectral emittance of the sun and earth.

To obtain the total scattering due to these effects one must integrate over the entire range of wavelengths and volumes of particles for any given condition at the time of imaging. It can be shown that the degradation of 'blue' (short wavelength) portions of multispectral data is amplified because of the high proportion of scatter in this region. Haze filters, such as Kodak Wratten filters, Number 90 series can be used to 'cut off' the short wavelength regions and hence also the amount of scatter (effectively noise) in wide-ranged spectrally sensitized films' image.

Scatter in the atmosphere also has the effect of lowering the contrast of the imaged scene [14] and we observe lowered contrast in short wavelength multispectral images

because of the increase in effective noise. (eg.In Landsat 4 series, band 1 data has a lower contrast than band 2, 3, or 4 ectera.)

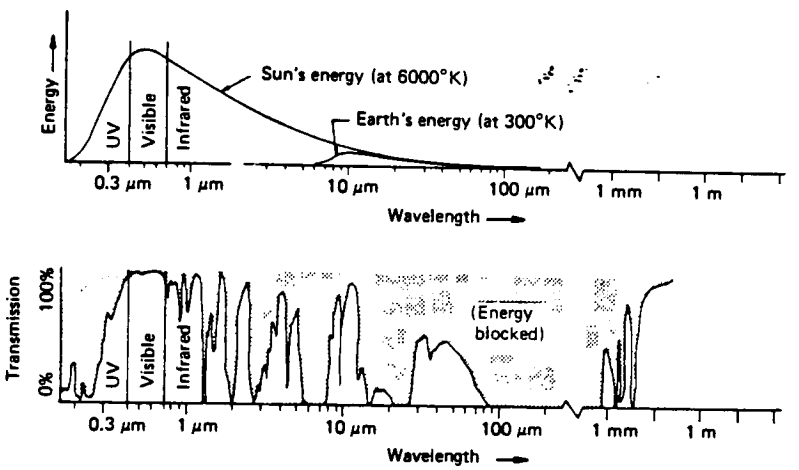

Figure 3 Energy Sources and Atmospheric and Atmospheric Transmittance

Various contrast processing techniques, notably contrast control, histogram stretching and false color coding therefore help in overcomming the effects of scattered radiation. Contrast control is changed photographically by various techniques. Developer type. developer temperature, processing time, agitation rate and different types of film are all parameters in contrast variations. Contrast stretching itself can entail the use of sophisticated image processing techniques which can lead to more interpretable imagery.

Photo-optical techniques most commonly used to enhance images fall into three distinct catagories; (1) Image sharpness, (2) Edge enhancement and (3) Contrast stretching [15]. Image sharpness can be improved in contact copy images

with the use of high quality Kohler illumination apparatus. Unsharp masking has been shown [15] to increase the definition of linear features where sharp density difference occurs. As mentioned, contrast control, mainly manipulated by film/developer combination or development time does enhance the visually interpreted result. The image can be density sliced and color encoded for display on a color CRT. Interpretation techniques can now be used to compare the various processes and their final product to the origional film with special attention to the ground feature of interest.

Landsat satellites have been in operation since July 1972. Four separate satellites have been placed into orbit providing various amounts of multispectral radiometric data to private and public sectors. With Landsat 4, (the most recent mission) new and better means of collection of data has been realized in improvement in ground pixel resolution and also expansion of spectral ranges as a Thematic Mapper (TM) has been included. The onboard multispectral scanners (MSS) record radiometric data in four discreet bands ranging from green to a mid-infared region and has ground pixel resolution of 80 meters per side. The TM data has seven spectral bands while the resolution is 30 meters in bands 1 through 6 and 120 meters in band 7. Images are transmitted to the ground and can be obtained as black and white, color composite images or computer compatible tapes. It has been shown that color

composite images of ratioed bands have significance in geologic discrimination. TM data ratios of spectral bands 4/1, 5/2 and 7/3 have been used with blue, green and red color additive illumination to produce high information color imagery. [17,18]

Landsat four (4) Thematic Mapper data is the premimum radiometric image source because of its superior ground resolution. Bands 4, 5, 6 and 7 for MSS imagery or bands 1, 2, 3, 4, 5, 6 and 7 for TM imagery are available to the civilian community as well as MSS data for Landsat 1, 2, 3. Photographic landsat images are accompanied by a 15 step gray scale to one side of the picture. The USGS-EROS Data Center in Sioux Falls, South Dakota utilizes a standard contrast index of 1.0 during photographic reproduction of standard Landsat images. [19,20]

Using the Landsat 3 MSS imaging system it has been shown that the r65 (infared to green) ratio best distinguishes between major material types such as water, soil, vegetation and rock but does not separate within group types. The r54 (red to green) ratio has been shown to distinguish within soil and rock groups and r76 (infared to red) ratio is best for delineation of vegetation types [21]. Problems inherent in the analysis of ratioed information are due to the fact that different materials can have different ground signatures and similar exposure ratios. Confusion as to the separation of

different ground feature is increased in this case. Some compromising statistical analysis have been developed to combat the problem digitally where the area of the image being investigated has been reduced to lower the probability of mixing two materials. [22] Having an 'a pripori' knowlege of geological types for classification, it is thought that the probability of mixing geological types will not be a problem.

Knowledge of the specific area of geological interest is of upmost importance. To understand parameters involved in spectral pattern recognition one must consider the conditions of the terrain or ground features to be sensed. The fundamental idea of remote sensing is the transformation of optically manifested results with attention to the transformation, application and dissemination of the information to physical quantity or parameter that is usable by some interested group. In this investigation, imagery should be obtained from an area with rock formations that satisfy a number of criteria:

Geologic Criteria

1. Diverse Geologic types
2. Nonflat Spectral Reflectivities
3. Horizontal Outcroppings
4. Minimum amount of biomass cover
5. Diffusely Reflective
6. Large spatial size

Any search for Landsat imagery of areas of geologic interest, as well as other applications, must consider a

number of system, sample and ground variables. Ground locations of Landsat imagery are defined using a World Reference (WRS) System that are related to longitude and lattitude points.

Geologically diverse sites in Utah have been used as test areas for analysis in rock discrimination.[23] An area south-south-east of Salt Lake City, encompassing seven, 50 square kilometers sites were used by Siegrest and Schnetzler because of its diverse geological content. Siegrest and Schneltzer, in their investigation, attempted to evaluate a number of spectral bands for their geologic content and attempted to separate a series of geologic groups based on their spectral reflectivities and emissivities. Optimum spectral bands in order of decreasing rock discrimination were found to be 1.18 to 1.30 micrometers, 4.50 to 4.25, 0.46 to 0.50, 1.52 to 1.73 and 2.10 to 2.36 micrometers. Hydrothermally altered rock, igneous as well as sedimentary rock types exist within the test area. With reference to geological survey maps it is shown that some of these rock formations are large enough to cover the resolution of Landsat MSS or TM systems.

Piech and Walker have worked with remotely sensed images for evaluation of surface texture and interpretation of soils, vegetation and water by using the aerial camera as an accurate photometer. Means were developed to accurately

measure, enhance and interpret color aerial photographic imagery. Evolved techniques divided color imagery into black-and-white separation transparencies with the use of band pass, "notch" filters. Band pass filters allow information from one spectral region through enabling the separation and recording of those regions. The combination of reflectance information from the two separated layers (usually red and green were used) resulted in a final ratioed image which was then analyzed for its information content with the use of a color encoded density slice machine. The work of Piech and Walker used color aerial photography as their information source. Separation of the color images resulted in some problems due to non-ideal notch filters that had finite transmissive bandwidths. Landsat imagery collects electromagnetic energy electronically with an oscillating scan mirror. The four on-board spectral detectors have very good spectral resolution and problems with finite bandwiths are reduced to a physical minimum.

Ratioed imagery is made within the remote sensing community for a number of reasons. Notably, the negation of various noise effects of system and ground variables have been identified and well investigated. The control of the contrast values of the raw images (before ratioing) has the ability to reduce scattered light effects [24] and improve the interpretability of the final ratioed image [25]. One

positive and one negative working contrast image are used for final ratio images. Mathematical prediction of the optimum contrast can be accomplished by relating the density difference of the final masked image in exposure space to corresponding reflectivity ratios of the ground features [26]. The basis for this method relies in the linear relationship between density and the log of the observed reflectivities. The human eye reacts to illumination on a log illuminance scale, therefore a log transmisson (of transparent images) or reflection relationship would be linear. The amount of illumination reaching the eye while viewing an image can be expressed as a function of the exposure (and the density) of that image. A quantification of the minimum perceived difference of illumination is necessary to show the ability of the human visual senses to percieve electromagnetic radiation. Density of a ratioed image is expressed as the sum of the contrast of the film times the log of division of the two spectral exposures. Density differences of a ratio image can be expressed:

$$\Delta D = \gamma_1 \text{Log} \left(\frac{X_1}{X_2}\right)^{\xi_1} - \gamma_1 \text{Log} \left(\frac{Y_1}{Y_2}\right)^{\xi_2} \qquad \text{[eqn 3]}$$

where X1,X2 and Y1,Y2 are the minimum and maximum exposures in each band, 1 is the original contrast of the image and 1 and 2 are the final process contrasts. With reference to Piech and

Walkers work a relationship for the exposure of a ground element of given reflectance can be found in using the alpha and beta calculation technique. Using a ground element that has a very low reflectivity, it can be shown that the minimum spectral exposure is an approximation of the noise or β term. Signal levels smaller than the noise can not be separated (or detected) and we see that sensed signal levels can be expressed as multiples of the exposure due to the noise. [appendix 6] Resulting density difference of two reflective elements can be expressed in exposure space as:

$$\Delta D = \gamma_1 \text{ Log } \left(\frac{X_1 - 1}{X_1 - 1}\right) - \gamma_1 \text{Log } \left(\frac{Y_1 - 1}{Y_1 - 1}\right) \qquad \text{[eqn 4]}$$

Once the two given relations are equated simple methods can be employed to solve for E1 and E2. Iterative methods involving the minimization of exposure difference minus reflectivity difference can be used and we note that quantification of the actual alpha and beta values is not needed (see appendix 5). The method involves inserting one previously obtained contrast value, (E2) with effective minimum and maximum geologic exposures into the equality and solving for the other contrast index (E1). It is hypothesized that this method could be compatable to actual fabrication of the separation masks using the original spectral band image and its contrast (E1) and a calculated copy contrast for the

other spectral band image. Ideal density differences of each feature in the resulting mask give separate, completely discernable reflectivity information.

Two spectral bands are needed that optimize the geologic information using the band ratioing technique. Two bands are needed that give exposures that are most different for all investigated rock types. One way to choose which two spectral bands are to be used in any one given ratio mask is to find which bands are least correlated in exposure space. Using spectral bands that are less correlated, we find that the ability to distinguish between actual ground signatures increases. Figure four shows two graphs that example low and high correlation of two spectral exposures for a number of features. Displays of exposure values in two 'best' spectral bands for a series of ground features about the equa-exposure axis shows an increased dispersion of those exposure values and the best ratioed differentiation between spectral signatures is realized.

Using a number of linear predictive equations as defined by a discriminant analysis and known spectral relationships, one can separate and catagorize unknown spectral exposures into a given set of ground features. A discriminant analysis essentially tries to form a linear combination of discriminating variables

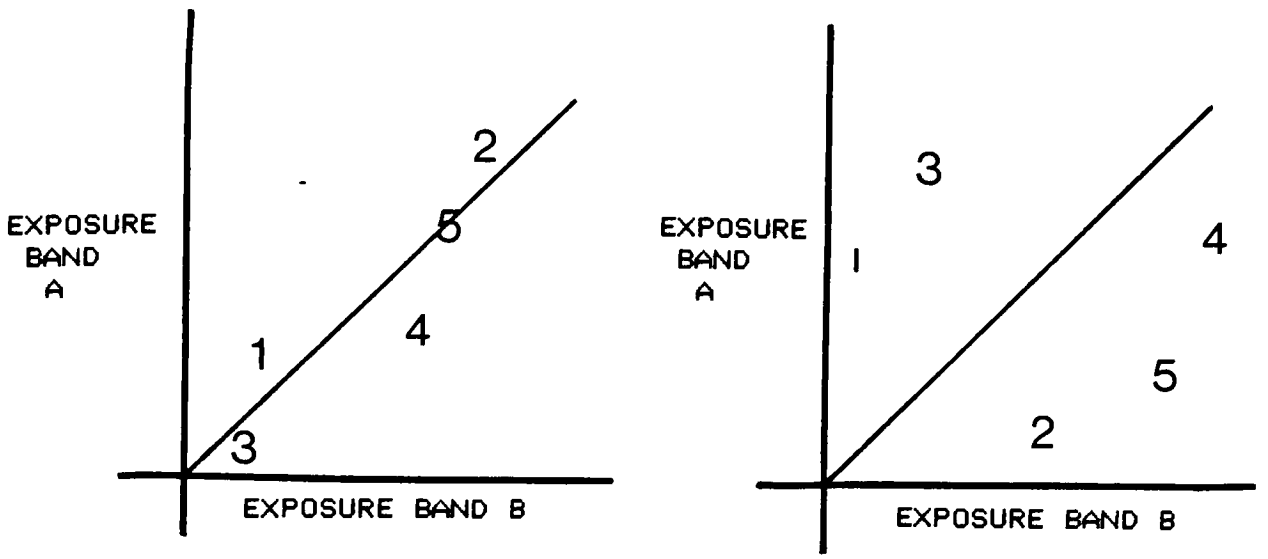

Figure 4 High and Low Correlation of Spectral Bands.

such that the largest group (rock types) differences and thus the largest discriminant criterion are observed. In exposure space, the distance between the group means is increased by the discriminant transformation and hence the ability to discern or separate groups is increased. By using this maximum separation of groups we are able to best distinguish between groups and knowing the coefficients for the mathematical transformation we can optimally classify groups with the best chance of success. The discriminating variables (spectral exposures) which are observed, enable the construction of discriminant functions. Once the discriminant function coefficients are found, a classification stage of unknown geologic types can be attempted. The discriminant scores are found for each unknown geologic type by entering spectral exposures into the equation:

$$D_i = d_{i1} Z_1 + d_{i2} Z_2 + \ldots + d_{ip} Z_p \qquad \text{[eqn 5]}$$

Where Di is the score on the discriminant function i, the d's are weighting coefficients and the z's are the spectral exposures. These discriminant scores are essentially euclidian distances from the unknown spectral exposure, in all four spectral bands to each of the groups. To classify a given unknown spectral exposure we choose the score with the smallest value (the smallest distance from the unknown point to the known group) and say that the unknown point is a member of the known groups distribution. Criteria for decision rules of this type of discriminant analysis only use the least exposure distance for catagorizing unknown data. Depending on the exposure spread or variance of the ground feature, be it due to spectral signature variations or other system variations, a given spectral exposure can be classified to varying degrees of success. Morrison [28] and Anderson [29] have both investigated the probablilties of misclassification under various degrees of knowlege of population parameters. Details of the determination of classification rules are documented by Anderson. Qualitatively illustrating possible misclassification, examination of frequency of exposure counts as a function of their exposure values (see figure 5) shows the variability and divergence of the individual exposures

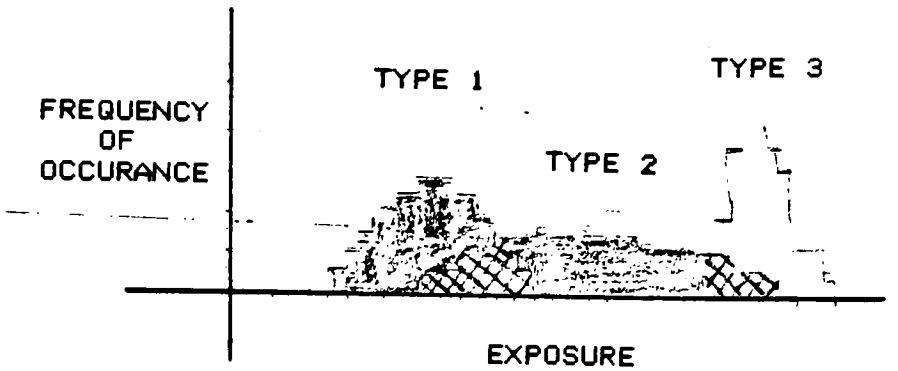

Figure 5 Frequency of Occurance vs Spectral Exposure.

for each ground feature.

To provide a statistical basis for spectral exposure and ground feature variances an analysis of varience can be used. Validity of exposure, geologic type relationships rely on the test of a null hypothesis. The hypothesis states that each of the two individual treatments (spectral exposures and geologic types) are each equivalent, meaning that the resulting spectral exposure from each of the unknown geologic types is the same. To state that each spectral exposure for geologic types is different it is necessary that we reject the null hypothesis and accept an alternative hypothesis. The ANOVA scheme calculates a series of test statistics which are distributed according to the F distribution. If calculated test statistics are greater than table distribution values then a conclusion that the two factors are independant and each of their effects are not equivalent is made. The data is

input into the design table in the form;

Factor A \ Factor B	1	2	...	b
1	$y_{111}, y_{112}, \ldots, y_{11n}$	$y_{121}, y_{122}, \ldots, y_{12n}$		$y_{1b1}, y_{1b2}, \ldots, y_{1bn}$
2	$y_{211}, y_{212}, \ldots, y_{21n}$	$y_{221}, y_{222}, \ldots, y_{22n}$		$y_{2b1}, y_{2b2}, \ldots, y_{2bn}$
.				
.				
a	$y_{a11}, y_{a12}, \ldots, y_{a1n}$	$y_{a21}, y_{a22}, \ldots, y_{a2n}$		$y_{ab1}, y_{ab2}, \ldots, y_{abn}$

NULL HYPOTHESES

Ho1 : t11 = t21 = ... = ti1 = 0

Ho2 : t12 = t22 = ... = ti2 = 0

Ho3 : (t11/t12) = (t21/t22) = ... (ti1/ti2) = 0

Table i. Two Factor Factorial Design Table.

where yij is each individual observation, u is the overall mean, ti is the treatment effect of factor A, Bj is the effect of the factor B, (tB)ij is the effect of the interaction between ti and bj, and eijk is a random error component.[31]

Here we have investigated tests that enable the testing of hypotheses that make conclusions about two treatments (spectral exposures and geologic types). To examine weather a number of individual observations of a single type of treatment (ratio mask exposure) are different another ANOVA test is necessary. Once a ratio image is fabricated, it is necessary to tell how well the image delineates geologic features based on densitometric measurements of the individual features. A one-way analysis of variance enables the

hypothesis testing by finding the ratio of mean squares of the treatment with the mean square of the error. A one-way design table (see table ii) sets up the data with a number of repeat observations for each treatment. The ratio of mean squares is a random variable closely distributed according to the F distribution and is tested against the distribution value with corresponding degrees of freedom for the treatment and error. Test F values that have smaller values than that of the table distribution imply that the mean square of the error is more dominant than that of the mean square of the treatments and any individual treatments are the same. Again we see that it is necessary to have larger values than the distribution values and reject the null hypothesis so each individual treatment/ratio image exposure of each rock type is different.

		Observation			
	1	y_{11}	y_{12}	...	y_{1n}
	2	y_{21}	y_{22}	...	y_{2n}
Treatment	.	.	.	...	.
	.	.	.	...	.
	.	.	.	...	.
	a	y_{a1}	y_{a2}	...	y_{an}

NULL HYPOTHESIS

Ho : t1 = t2 = ... = ti = 0

Table ii. One factor Design Table.

Optimum spectral bands for deliniation of rock formations have been investigated (Holmes, Nuesch, Vincent [23] and Segriest, Schneltzer [30]) for use in the application

of geologic problem solving. Systems that have been used have been based upon the ability to detect specific geologic types via their spectral reflectance and spectral emittance characteristics in the near infared and mid infared spectral region. Segriest and Schneltzers' in their investigation used a stepwise discriminate analysis on remotely sensed data from a 24 channel Bendex MSS to separate rock materials and to order each of the bands as to their usefulness. Their work however was not applicable to ratioed imagery classification of geologic types as the results only showed relative discriminatory power of individual spectral bands. Investigations such as these give indications as to what types of sensors and spectral bands are used for given geological surveys and provide imputes for proposed work.

EXPERIMENTAL

The proposed project consisted of testing the ability of the discriminant analysis with ratio imagery to identify, predict and confirm geological features on the basis of densitometric information of a given Landsat multispectral scene. The 'a priori' knowlege of geologic types and their spectral exposures on the MSS image provides the data for this investigation. With these existing guidelines resulting information of this project will be limited to the given scene and therefore will have limited use for other sources of data other than provide general guidelines and trends. However, if proper radiometric calibration of other scenes with the tested scene is possible, then the calibration between known and unknown exposures is possible and generated information will be compatable. The scope of the proposed work is to provide a context or foundation of experimental procedures enabling the classification of natural geologic features and types using ratioed Landsat imagery.

Test Imagery

To test the ability to distinguish between rock types from the Landsat orbital platform, it is necessary to previously run a series of lab tests to provide proper

justification. Test data that is comparable to the Landsat photographic imagery was acquired in the following manner. Using Kodak High Speed Infared Film 2178 and four combinations of Kodak filters, 92 &103, 93 & 103, 94 &103 and 87C, we can nearly approximate the discreet spectral bands of the MSS sensor. The spectral transmittance of these filters are plotted (see figure 7), and are generally close to that of the Landsat MSS detectors sensitivity. Landsat sensors are sensitive as follows: band 4 0.4-0.5um, band 5 0.5-0.6um, band 6 0.6-0.7um and band 7 0.8-1.1um.To obtain imagery, a set of geologic samples were needed.

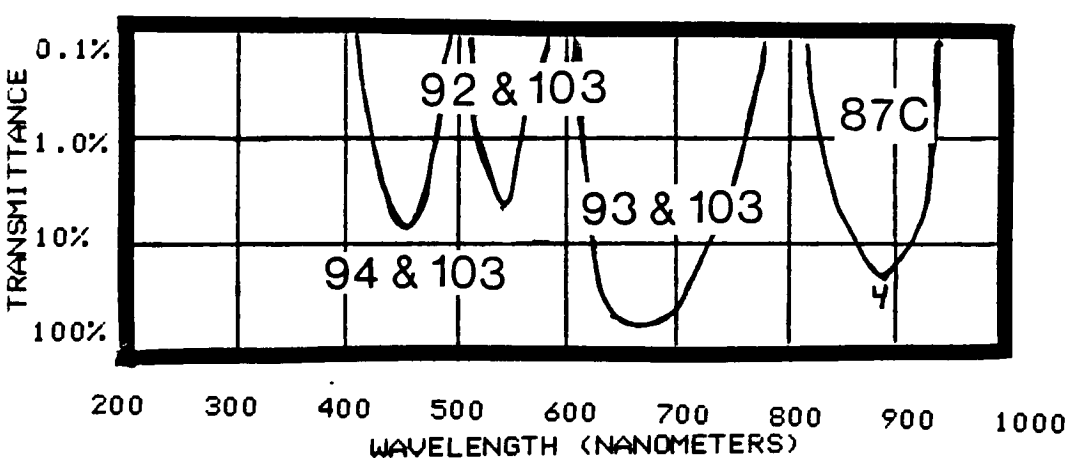

Figure 7 Imaged Spectra using 2178 Film and Several Filters.

If the origional objective of this analysis is to separate specific geologic types for an individual survey, then samples of these types should be used for the test imagery. Spectral

ground truth data would then enable quantification of many atmospheric and sensor effects (such as o and B). In a general, non-specified experimental approach, a set of any rock samples can be used. In this case, no comparison can be made between final Landsat geology and the test results, only general methodology is tested. A reflection step wedge was imaged in all four spectral bands with the rocks on an 18% gray card (for control). As the imaged rocks are of fairly large size on the film, a diffuse densitometer, such as the McBeth TD-100 was used to obtain densitometric information. The imaged step wedge allows proper log exposure calculation from each spectral bands' contrast value. These log exposure values are converted to exposures (raise to the base 10) and following analysis can begin. It is noted that a similar exposure data collection approach is used for the final Landsat scene. The only difference entails the calibration and configuration of a microdensitometer. It is necessary to calibrate diffuse transmission densities as measured by the McBeth to the output of the microdensitometer. The RIT/Calspan Roscoe microdensitometer has gain and zero adjust for this calibration purpose.

Microdensitometer Configuration

The Multispectral Sensor aboard the Landsat series 1,

2, and 3 satellites has a ground element resolution of approximately 80 meters per side. Using an image with scale of 1:1,000,000 and the given ground resolution the image element size on the film would be 80 microns per side. It is hypothesised that a microdensitometer configured to 80 micron aperture diameter would be able to closely resolve the minimum ground distance as limited by the imaging parameters.

Landsat Imagery

This projects origional intention was to investigate (general) rock types, and test for their discriminatory power within the ratioed image. With intention of investigating general rock types to test general theories, proper ground test sites are needed with proper imagery. The Landsat series imaging platform was chosen as the data base and a number of restricting guidelines must be followed because of system limitations. In attempting to evaluate the proposed system a ground area must be found that has diverse geology. Landsat imagery of this ground area must then be obtained. The Earth Resources Observation Systems (EROS) program of the U.S. Department of the Interior administered by the Geological Survey provides remotely sensed high altitude and satellite data to the general public. Areas of ground locations are correlated to a Landsat coverage index and World Reference

System coordinates are found. A computerized search for the ground imagery results in a list of parameters involved in the acquisition of the images. In this investigation the search priorities are as follows:

Search Priority Structure

1. Image/Groung Location
2. Type of Imagery
3. Image Quality
4. Cloud Cover
5. Exposure Date
6. Image Size (scale)

To provide a basis for the relationship of geologic ground feature and its resulting exposure on the photographic multispectral scenes one may examine an Analysis of Variance (ANOVA) scheme. A two-way ANOVA has the ability to test hypotheses,

Source of Variation	Sum of Squares	Degrees of Freedom	Mean Square	F_0
A treatments	SS_A	$a-1$	$MS_A = \frac{SS_A}{a-1}$	$F_0 = \frac{MS_A}{MS_E}$
B treatments	SS_B	$b-1$	$MS_B = \frac{SS_B}{b-1}$	$F_0 = \frac{MS_B}{MS_E}$
Interaction	SS_{AB}	$(a-1)(b-1)$	$MS_{AB} = \frac{SS_{AB}}{(a-1)(b-1)}$	$F_0 = \frac{MS_{AB}}{MS_E}$
Error	SS_E	$ab(n-1)$	$MS_E = \frac{SS_E}{ab(n-1)}$	
Total	SS_T	$abn-1$		

Table iii. ANOVA Table for the Two-Way Classification Model.

Ho: Ti=0 (no spectral band factor effects), H0: Bi=0 (no geologic type effects), and H0: (TB)ij=0 (no interaction effects).

Calculated test values that relate the mean square of each of the treatments and interaction to the mean square error within treatments is a random varible with the F distribution. The calculated test values Fo(A), Fo(B) and Fo(AB) are compared against a test statistic, book value of the F distribution for a given confidence coefficient and degrees of freedom. To prove relationships between rock type and spectral exposures we must reject null hypotheses and accecpt the alternative hypotheses.

Discriminant Analysis

To distinguish between geologic types a discriminant analysis is used. The Statistical Package for the Social Sciences is a system of computer programs that has been developed for use in several disciplines. The discriminant analysis routine provides a number of statistical methods to test the discrimination between a number of groups.

Correlation analysis coefficients describe the degree of association between the two variables. (see appendix 4) As four spectral bands are accessed, two must be choosen that best represent the geologic groups. Criteria for the chosen

spectral bands are that they both have low correlation and high discriminatory power. Using the SPSS Discriminant analysis subroutines, we choose the two spectral bands that have the least pooled correlation values. These two spectral bands exhibit a low linear relationship between their exposures.

Two major research objectives of the discriminant technique are analysis of known data and classification of unknown data. Once a set of discriminant functions are found that provide maximum possible discrimination for cases of known memberships, a set of classification coefficients are derived which allow the classification of unknown cases. Discriminant scores are found for a series of unknown geologic spectral exposures enabling the delineation of each group. A confusion matrix is used to visually diagram the sucess of the discrimination for all known geologic types. The aforementioned unknown geologic groups are simply taken as a random sample of the known groups and tested as such. Classification of these groups actually tests the performance of the discrimination functions. The basis of all spectral pattern recognition relies on the fact that spectral change within the tested ground elements exists. If the physical phenomenon of change in reflectivities across the electromagetic spectrum did not exist, initial investigation would show this in the two-way ANOVA as a falure to reject

null hypothses.

Contrast Calculation

Two multispectral images are chosen that best describe the spectral exposure differences of the geology and an experimental technique is needed to calculate the contrast values that best represent the data as reflectance ratios observable by the eye. Density difference as observed by the eye is related to the reflectance ratio. Knowing maximum and minumum exposures of the test geologic types and the origional contrast of one of the chosen spectral bands, the process contrast of the other chosen spectral band can be found.

$$\xi_1 = \mathrm{LOG}\left(\frac{X_2}{X_1}\right) + \mathrm{LOG}\left[\mathrm{ABS}\left(\frac{X_1-1}{X_2-1}+\frac{Y_1-1}{Y_2-1}-10^{\xi_2}\left(\frac{Y_2}{Y_1}\right)\right)\right]$$

Production of Ratio Image

The production of the ratio image is enabled by the culmination of the disriminant analysis and the contrast calculation scheme. Once two spectral bands are chosen for the ratio mask that optimize spectral difference information, other bands can be ignored. One spectral band is chosen as the "original" band and that contrast value with the minimum and

maximum spectral exposures, (of the two bands) X1, X2, Y1 and Y2, are input into the contrast calculation equation. A process contrast value is found and the mask can be made. The ratio image is made by registering the positive and negative masks. Now the resulting image can be density sliced. An analysis of the optimum ratio image as a geologic information source can now be made.

Analysis of Ratioed Imagery

Once the ratio image is produced, it is necessary to investigate its discriminatory power as an information carring source. A set of densitometric data is taken of the geologic areas of interest from the ratio image and means are needed to test if exposure measurements from an individual rock type is different than the next. As we've seen in the analysis of rock type, origional MSS exposure ANOVA test, the test for the set of hypotheses will prove the ability to separate rock types given a set of exposures. Using the same criteria as before, only having one factor (geologic ratio image exposure) and a number of observations per factor, the hypothesis that the geologic types are different is tested using the one-way ANOVA scheme.

Source of Variation	Sum of Squares	Degrees of Freedom	Mean Square	F_0
Between treatments	$SS_{\text{Treatments}}$	$a - 1$	$MS_{\text{Treatments}}$	$F_0 = \frac{MS_{\text{Treatments}}}{MS_E}$
Error (within treatments)	SS_E	$N - a$	MS_E	
Total	SS_T	$N - 1$		

Table iv. ANOVA Table for the One-Way Classification Model.

A rejection of the null hypothesis that says that each of the geologic groups are equivalent, is necessary to conclude that they are different.

RESULTS

1. Two-Way Analysis of Variance Results:

TEST IMAGERY

SOURCE OF VAR	SUM OF SQUARES	DF	MEAN SQ	F(0)	test F(o)
A	23681645.3	6	3946940.8	7610.92	2.20
B	993945.5	6	3946940.8	751.28	2.20
AB	5419835.74	18	301101.98	46.6	1.71
ERROR	723589.03	112	6460.61		
TOTAL	30819015.5	139			

SCENE 21685- 17255

SOURCE OF VAR	SUM OF SQUARES	DF	MEAN SQ	F(0)	test F(o)
A	86926.44	9	9658.49	4421.08	1.97
B	8922.4	9	9658.49	1361.38	1.97
AB	9687.77	27	358.8	164.24	1.57
ERROR	611.69	280	2.18		
TOTAL	106148.32	319			

2. Discriminant Results

- Discriminant Function Coefficients

TEST IMAGERY

CLASSIFICATION FUNCTION COEFFICIENTS
(FISHER'S LINEAR DISCRIMINANT FUNCTIONS)

CASE =	1	2	3
SB1	0.3677126	0.2308188	3.227931
SB2	0.4291953	0.2392840	4.230538
SB3	0.9672330E-01	0.5040152E-01	1.075419
SB4	1.517139	0.8755617	15.36907
(CONSTANT)	-111.5702	-40.68310	-1044.40

4	5		
0.7161959E-01	0.5423140E-01	0.1452468	[illegible]
0.5913771E-01	0.5698332E-01	0.1334783	[illegible]
0.1402910E-01	0.1327990E-01	0.3124582E-0[illegible]	[illegible]
0.2521608	0.2169913	0.5386050	[illegible]
-5.488410	-4.179917	-16.57582	[illegible]

SCENE 21685-17255

CLASSIFICATION FUNCTION COEFFICIENTS
(FISHER'S LINEAR DISCRIMINANT FUNCTIONS)

CASE =	1	2	3	4
SB1	41.42080	2.445969	1.304113	10.26858
SB2	24.10017	2.354551	0.4196826	8.610551
SB3	29.63526	3.100205	2.174952	9.108128
SB4	27.49313	3.976699	2.972473	10.09824
(CONSTANT)	-3741.138	-41.53872	-17.36181	-384.3654

5	6	7	8	9
6.741384	5.398363	1.453497	7.227035	5.898256
5.136962	4.958760	0.7137084	9.100269	6.261506
5.724699	5.689773	2.947786	8.759228	6.654990
5.574644	5.602312	3.650274	9.890899	7.473438
-143.0395	-130.4322	-26.97509	-358.2398	-194.9814

10	11	12	13	14
2.103943	3.328717	2.397875	1.894823	6.243293
2.870257	3.016160	1.006753	1.809856	4.882276
2.423543	3.819105	3.729117	3.356062	5.609560
3.198227	4.547771	5.521905	5.404894	6.096907
-35.99138	-61.04256	-50.61158	-49.74607	-138.0556

15	16	17	18	19
7.231001	6.293146	1.653046	2.610481	2.495498
6.794939	5.529025	1.140494	2.139080	2.251583
7.222248	5.236786	2.260619	3.363868	2.627587
7.890384	5.663480	3.426012	4.991043	3.735338
-232.5567	-141.2823	-23.04434	-50.06895	-35.87356

- Correlation Results

TEST IMAGERY

POOLED WITHIN-GROUPS CORRELATION MATRIX

	SB1	SB2	SB3	SB4
SB1	1.00000			
SB2	-0.05719	1.00000		
SB3	0.31024	-0.20832	1.00000	
SB4	-0.57767	0.01473	-0.44406	1.00000

SCENE 21685-17255

POOLED WITHIN-GROUPS CORRELATION MATRIX

	SB1	**SB2**	**SB3**	**SB4**
SB1	1.00000			
SB2	0.11346	1.00000		
SB3	-0.12467	0.05048	1.00000	
SB4	-0.00596	-0.00192	-0.13521	1.00000

3. Classification of Known Geologic Types. Confusion Matrix (Percentage Classified)

TEST IMAGERY (5 data points)

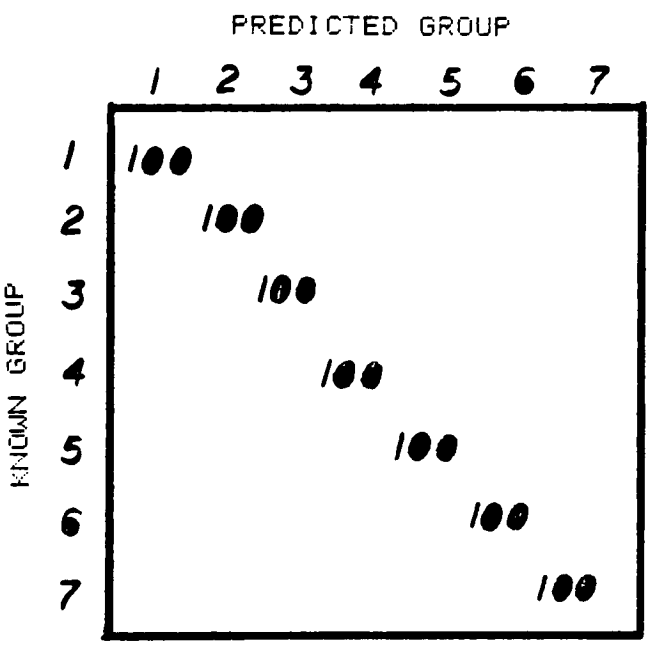

SCENE 21685-17255 (19 data points)

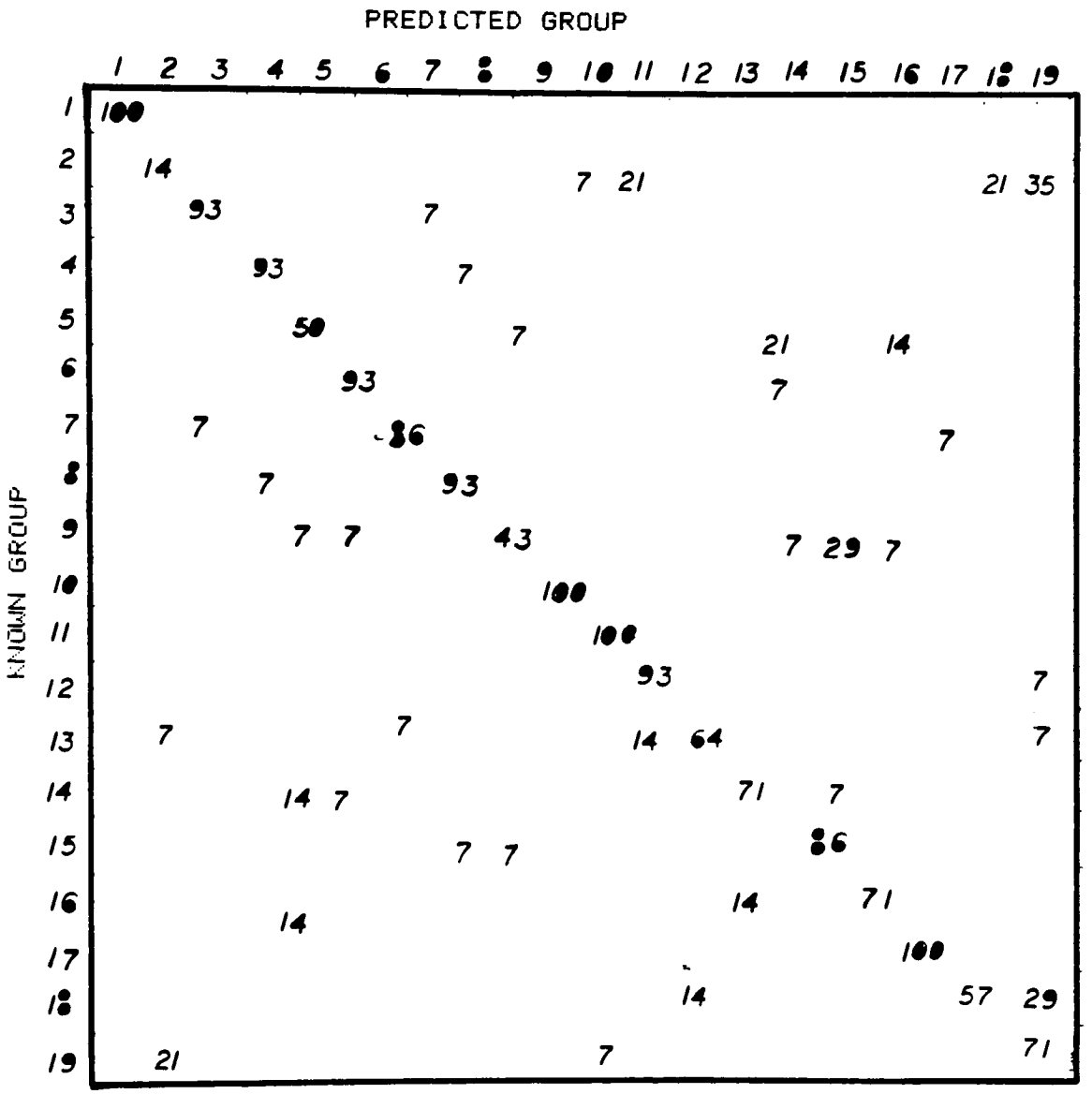

4. Contrast Calculation

TEST IMAGERY SCENE 21685-17255

SPECTRAL BAND	2	4	5	7	
MAXIMUM EXPOSURE	115	794	92.6	48.6	LUX-SECONDS
MINIMUM EXPOSURE	2.24	204	0.995	3.68	

ORIGINAL CONTRAST OF
SPECTRAL BAND 2 = 0.33

CALCULATED CONTRAST OF
SPECTRAL BAND 4 = -0.48

ORIGINAL CONTRAST OF MSS
SPECTRAL BAND 5 = 2.25

CONTRAST OF COPY (POSITIVE)
OF SPECTRAL BAND 5 = 1.[illegible]

CALCULATED CONTRAST OF
SPECTRAL BAND 7 = -2.30

5. Classification of Unknown Data. Confusion Matrix (Percentage Classified)

TEST IMAGERY (1 data point)

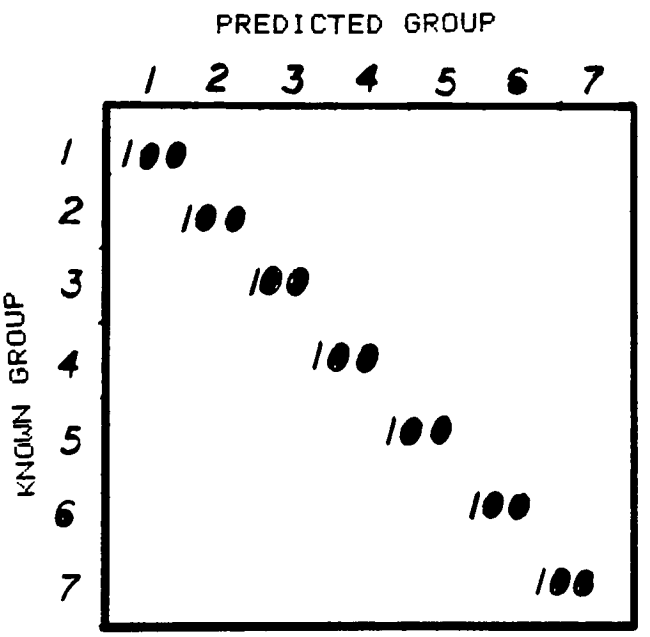

SCENE 21685-17255 (2 data points)

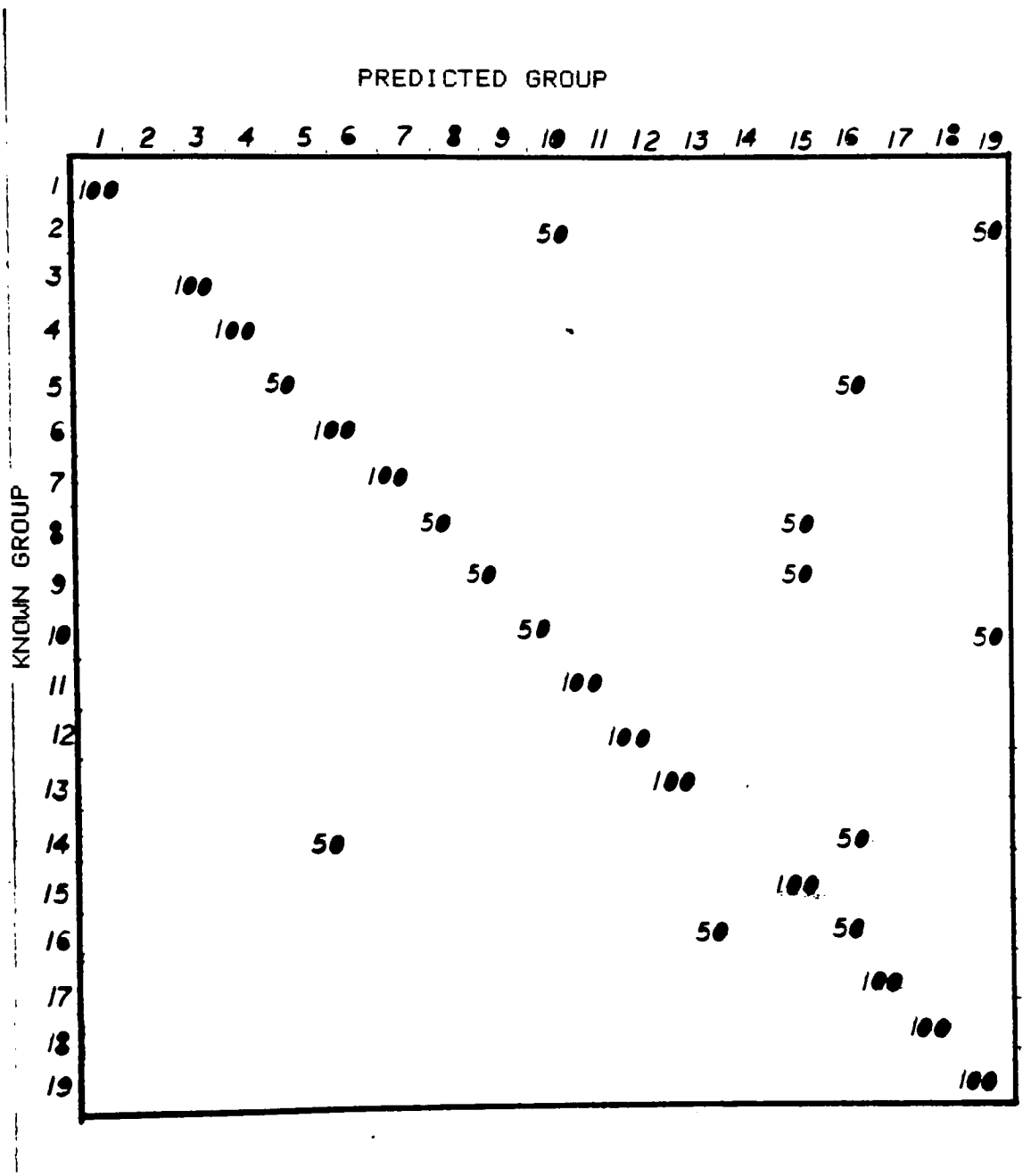

6. Mean Spectral Exposure Values fo Geologic Types of Original Multispectral Imagery

TEST IMAGERY

CASE	SB1	SB2	SB3	SB4
1	235.96000	105.92800	130.12000	[illegible]
2	182.88000	56.99000	15.61[illegible]00	[illegible]
3	1035.87999	940.06000	2164.60000	[illegible]
4	69.74800	15.02600	24.10400	[illegible]
5	38.23200	11.67600	17.01600	[illegible]
6	124.90600	22.11200	35.60600	[illegible]
7	8.05000	2.58000	3.31600	[illegible]
TOTAL	242.23657	164.91114	341.[illegible]	[illegible]

SCENE 2165-17255

CASE	SB1	SB2	SB3	SB4
1	46.17000	90.32857	74.03571	43.39214
2	2.59450	8.50157	7.79814	6.70136
3	1.07196	1.94714	5.31457	5.06671
4	11.58193	31.05214	22.97571	16.56429
5	7.55979	18.70714	14.58357	8.90500
6	5.97079	17.84071	14.75429	8.98321
7	1.12359	3.03407	7.42236	6.13193
8	8.24336	31.89571	22.78071	16.29929
9	6.59364	22.24286	17.12500	12.30257
10	2.47457	9.96843	6.18293	5.40643
11	3.59057	10.91193	9.66586	7.56793
12	2.08457	4.28693	8.98036	9.51321
13	1.76400	6.67871	8.14193	9.40786
14	6.94850	17.76643	14.14357	9.96586
15	8.12043	24.32000	18.46357	12.91500
16	7.23800	19.78214	13.25643	9.23971
17	1.61000	4.33143	5.45464	5.91579
18	2.66793	7.88714	8.18557	8.59100
19	2.74157	8.11164	6.43179	6.38564
TOTAL	6.84998	17.87341	15.03667	11.01342

7. One-Way Analysis of Variance Results.

SOURCE OF ERR	SUM OF SQUARES	DEG. FREE.	MEAN SQUARE	FO	test F(o)
TREAT.	38828.761	18	2157.153	379.95	1.69
ERROR	755.099	133	5.677		
TOTAL	39583.86	151			

8. Ratio Image Reproduction

SCENE 21685-17255

9. Resultant Densities of Ground Sites for the Ratio Mask, (eight points per site) Scene 21685-17255

Site	Name	Average D	Std. Dev
1	Lake Deposits	1.05	0.02
2	Miocene Volc.	1.46	0.04
3	Oligocene Volc.	1.36	0.02
4	Basalt & Rhyolite	1.12	0.03
5	Basalt & Rhyolite	1.16	0.01
6	Old Alluvial Dep.	1.19	0.02
7	McCoy Cr. Groups	1.50	0.03
8	Temple Bu. Form.	1.18	0.03
9	Miocene Volc.	1.12	0.03
10	Landslides	1.40	0.02
11	Navajoe Sandstone	1.26	0.03
12	Quartzite	1.57	0.04
13	White Sage Fm.	1.53	0.06
14	Alluvium & Colluvum	1.13	0.01
15	Lake Deposits	1.04	0.02
16	Miocene Volc.	1.11	0.03
17	Basalts	1.50	0.01
18	Cretaceous Fm.	1.28	0.03
19	Arapian Shale	1.92	0.03

DISCUSSION OF RESULTS

The two-way factorial analysis of variance was investigated using the laboratory test imagery. Five rock types out of the imaged 12 were not used because of their very irregular surfaces and therefore point-to-point variability of exposure. Five log exposure points were taken of each of the seven rocks with the McBeth densitometer in all four spectral bands. Densities were very uniform of the seven rocks investigated and it was thought that five samples was sufficient. Because of the non-discreet cut off glass and wratten filters, it was noted that error within classification processes might be introduced. The 92 & 103, 93 & 103, 94 & 103, and 83C filters were chosen because they most closely approximate the discreet bands of the Landsat multispectral sensor system. Results of the two-way ANOVA gave indication as to whether any of the seven rock types were equivalent for their varying spectral exposures. The test statistics Fo(A), Fo(B) and Fo(AB) proved that each rock type did give a distinctly different exposure and there is significant interaction between geologic classes and spectral exposures. The rejection of all three null hypotheses with Fo(A)=610.9, Fo(B)=51.28 and Fo(AB)=46.60, gave the main impetus for further investigation using high altitude,

small scale imagery.

The laboratory test data was now subjected to the outlined experimental procedure. The discriminant analysis' correlation matrix of spectral bands showed that band 2 (spectral region corresponding to the 92 and 103 filters) and 4 (region corresponding to the 87C filter) were the least correlated, having a correlation of 0.01473. Using the contrast of band 2 (0.32), the lowest and highest exposures in band 2 and 4, and the contrast calculation program it was found that the optimum copy mask contrast of spectral band 4 was 0.48. This indicated that a geologically optimized ratio mask could be made using a positive image of band 2 and 4 with contrasts of 0.32 and -0.48. SPSS software on a Vax 11780 ran the discriminant analysis and 100% of the dependent, known data was classified into their corresponding groups as is shown by the confusion matrix of test imagery. An independent set of data was used to test the discriminant function classification of the test imagery. One series of spectral exposures from each rock sample was input in the discriminant functions and all five were catagorized correctly. It is noted that the seven rock types were chosen by chance and employed to prove, via the ground level imagery approach, that the processes work. Comparison of the calculated parameters from these test images have no

meaning in the evaluation of space born imaging systems, other than that the projects' hypothesis is valid and justified.

Ground areas of interest were identified for their feasability in this study. Areas in Southern Utah and Death Valley, California comprised the main sites of investigation. An area south, south east of Salt Lake City, Utah proved to be sutiable. The location encompases an area of approximately 360 square miles, with diverse geologic content. Geologic groups within the area include;

Lake bed Deposits	Basalts
Miocene Volcanic Rocks	Arapian Shale
Oligocene Volcanic Rocks	Quartzite
Basalt and Rhyolite	Sandstone
Alluvial Deposits	
Older Alluvial Deposits	
Alluvium and Colluvium	
Cretaceous, Kaiparowits Formations	

Visual verification of United States Geological Survey maps [35,36] showed that the geology was of large size and diverse types. A search of Landsat 4 imagery was first investigated of this area using the Search Priority Structure Guidlines. The image/ground location was of

utmost importance in the search overshadowing all other parameters. It is noted however that the quality of the Landsat scene must be maximized to enable the best measurement of the spectral exposures. Specific imagery parameters requested were as follows: MSS imagery of path 41 and row 33 (of World Reference Frame coverage), image quality no less than 8 for all spectral bands (on a 1 to 10 scale), 0 % cloud cover, exposure date between September and November and image size to permit a scale of 1:1,000,000. The first search for the imagery gave ground locations that were too far north east of the the site. A second search for the test site shifted to cover the test area, however the image quality, cloud cover and exposure date all prohibited the use of this and all existant Landsat 4 imagery. A downgrade to Landsat 1,2 or 3 imagery was necessary in an attempt to obtain the most usable imagery possible. Landsat Satellite 2 image 21685-17255 was found, on this third search, to be the best set of spectral images and were then obtained. The areas covered within the test site of landsat image 21688-17255 are:

Area of Landsat Image 21685-17855

	Latitude	Longitude
corner 1	N39D17M30S	W111D24M04S
corner 2	N39D36M48S	W113D24M34S
corner 3	N38D12M30S	W113D52M45S
corner 4	N37D53M12S	W111D54M35S

Sixteen density points were taken of nineteen

geologic groups in each of the four positive contrast spectral bands 4, 5, 6, and 7. Four of the geologic groups were repeated once within the nineteen groups. This was done on the grounds that an 'a priori' knowledge of the spatial separation of each group was well known. A classification of an unknown data point thought to be of one of these repeated types, is constrained by ground location requirements. If a spectral measurement is classified into one of these groups and it is known that the measurement was not close to that group then the probability of correct classification would go down.

The Roscoe Microdensitometer was configured to a 75 micrometer aperture diameter (75 meters on the ground) and output calibrated to maximum and minimum diffuse densities on each multispectral 15 step exposure wedges. Proper image registration of each density measurement on the microdensitometer was needed so as to receive reflectivity information of the same element. Visual cues from the ground maps and the imagery were used as sole references for density measurement. Prominant lakes, mountain formations, gullies and such enabled registration for most measurements. An electronic positioning system such as a plotting table with X, Y coordinate readouts attached directly to the microdensitometer would enable better registration and this is suggested for future work. Density

measurement would be more precise and reflectivity information (in the form of densities) would be more accurate. In instances where little or no visual cues exist in the image a clear overlay with small holes for measurement would also help.

The densities were converted to relative log exposures via the images' characteristic curve. The Roscoe microdensitometer is calibrated using gain and zero adjust knobs and its output is linear with respect to density. Characteristic curves are essentially a straight-line conversion form density to exposure. The four spectral characteristic curves each had a slope of very close to 0.75 and log exposures were converted to exposures. Fourteen of the sixteen individual spectral exposure values were used in the analysis phase of the discriminant analysis and two were witheld for use as an independant test set. The dependant data was translated into a SPSS discriminant analysis command file (appendix 5) and all of the nineteen geologic groups were included in the initial investigation. It was found that the Landsat spectral bands 5 (red) and 7 (far infared) were least correlated. Their pooled correlation was -0.00192 and this indicated that these two spectral bands have the least amount of interdependant geological information for these rock types and most widely vary in their spectral exposures. These two

spectral bands, 5 and 7 were used in the ratio image fabrication.

The SPSS routine generated a number of classification functions for the dependant data set and corresponding classification coefficients. The classification results of the dependant data set gave 77.82 percent correctly classified. Several groups poorly classified their data. Group 2 classified only 14% and groups 5, 9 and 18 classified under 60% correctly. (see confusion matrix of dependant data) The somewhat poor level of 78% classification is because of inferior classification of these groups. Groups 3, 4, 6, 7, 8, 10, 11, 15 and 17 all classified above 85% of their geologic features. It is noted that 14 spectral exposure measurements for each rock type was taken and the minimum possible percentage missclassified was 7.1 percent. To enable classification of rock types that provides a good approximation of the population of spectral exposures a minimum of approximately 30 points should be taken.[37] To enable higher classification accuracy of rock types, it is thought that the use of several discriminant function routines could help possibly including other gelological defining parameters. Depending on several variables including ground pixel element size, it may be possible to add a texture variable to the discrimination functions. For example, it

may be found that the texture of one or more groups is significant and measurable in a given spectral band. A variable that is in direct relation with texture can then be included. Investigation of the separation of groups in exposure space cues the observer into which groups will be best classified. Using a number of generations of discriminant functions with groups that are close to one-another, it may be possible to increase classification efficiency. Very good knowlege of exposure data for tested geologic types is necessary for this method and a large sample of data is an absolute must. It is thought that an accuracy of at least 99 percent could be sufficient for field work.

Initial classification of the independant data was attemped with the calculated set of discriminating functions. The two spectral exposure measurements that were not used in the generation of the discriminant function coefficients were used to test the ability of the system to classify unknown rock types. The series of two spectral exposures were included in the SPSS command file at the bottom of the file stack. Each of the two sets of exposures were classified by calculating discriminant scores for each rock type and classifing a given spectral exposure into the score with the lowest value. Seventy six percent, or 29 of the 38 spectral measurements were catagorized correctly and

it was shown that in a test situation, one could correctly classify geologic groups by spectral exposure measurements. (see unknown classification results)

Having established the lack of correlation between bands 5 and 7 the geologically optimized ratio mask was made. A copy of band 5 was made (negative) and then copied again to give a duplicate of the original. Using the contrast of the copy of band 5 (1.96) and maximum and minimum exposures of the original band 7 and the band 5 image the unknown contrast value for the copy negative of band 7 was found. The calculated contrast of the band 7 image was found to be 2.29. The final ratioed image was made by the overlay of the positive image of band 5 and the negative of band 7. Eight density points were now taken of each of the 19 ground areas of the ratio image and the final analysis was undertaken.

A one-way analysis of variance was then used to test the individual treatment (geologic group mask exposure) interdependencies. Eight density measurements of the overlayed image for each site was taken. These density points were converted to a reflectivity ratio quantity by raising the mask density to the power 10. Reflectance ratio were inserted into the one-way ANOVA program with eight observations and nineteen treatments. The resulting F value which is a variable distributed according to the F

distribution was calculated to be 380. We see that this is much larger than the book value for 99 degrees of confidence (and degree of freedom of 18 and 151) of 2.00. The Fo value is was so high because of the variablilty of the densities (of the features) on the mask. With reference to the standard deviations of the density values (see results) we see that they are of relatively small magnitude. This small flucuation (individual treatment variation) gave a small sum squares of error and a resulting large Fo. The small variation does not seem to encompass variability that should exist within the features, only variability of measurement itself. Reasons for this may be of a human interaction nature. Density measurement of many of the features with the microdensitometer used is very subjective. Errors, or lack errors within the densities may be the observers fault impressing a judgment on the data. A non-objective measurement technique such as a scanning microdensitometer or digital images with computer manipulation simply would take care of this. So we conclude that measured density of the ratio mask image has the ability to discern reflectivity difference information of the investigated ground locations with this landsat multispectral scene. The visualized density of the ratio mask, in the form of a reflectance ratio may not necessarly be able to discern

between geologic groups even though measured differences can. Application of techniques using the minimum change in density as seen by the eye (this has been well established) for all geologic groups would enable an investigation as to how well the eye can separate groups of interest. This is suggested for future work.

CONCLUSIONS

Using high altitude imagery accuired by the Landsat 2 satellite system it was found that there was a difference in mean spectral reflectivity of a number of tested geologic types. A two-way analysis of variance using spectral exposure data in the four spectral bands 4, 5, 6, and 7, gave the conclusion that each tested geologic group differed with a confidence limit of 99 percent. Calculated F numbers for the observation (FoA), treatment (FoB), and interaction (FoAB) each showed that there was significance within the effects all three variables. Confirmation of the significance of a geologic type, spectral exposure dependance provided a basis for the discriminant and ratio analysis.

The discriminant analysis program provided correlation coefficients enabling proper fabrication of an optimized ratioed image and spectral classification routines. A correlation analysis gave the two spectral bands that were most orthogonal in their representation of the exposure data. These two spectral bands 5 and 7 were used in the fabrication of the ratio image which allowed testing of this ratio image for its separation power of geologic types. A one-way analysis of variance tested the hypothesis that the reflectance ratio of the two spectral

bands is different for the geologic types within the fabricated ratio image. The calculated test value of Fo was 380 and it was thought that this very high magnitude was due to the lack of measured exposure difference within each geologic group. The results did show trends within the photometric processing, ratio mask fabrication technique, concluding that each geologic group had distinct measured differences. It was thought that digital techniques with their objective measurements would more faithfully record exposure differences of a ratio mask and would therefore effectivly lower the test Fo value. The inherent subjective measurement of densities using the Roscoe microdenditometer was a problem as actual measurement may have been modified by the observer.

A discriminant analysis was performed to attempt a classification of the geologic groups with spectral information in all four spectral bands. The analysis transformed the spectral information into a new set of variables that maximized the distance between geologic groups and enabled a classification accuracy of 77.82 percent for the dependant data set. The classification accuracy of 77.82 percent was caused by poor separation of a few geologic groups and this deflated the overall ability to classify known and unknown groups. It was hypothesised that individual group classification accuracy (accuracy

being based on the generation of the discriminant functions for the dependant data) more justly shows the separation and classification ability of each geologic group. The dependant data set consisted of 14 exposure measurements for each of the 19 tested geologic groups which was felt to be a good representation of the distribution of spectral exposures. Repetition of four alike groups were used in the discriminant analysis and were treated as separate ground features. Further analysis of these four geologic groups is heavily dependent on the ground location and it was thought that this could lower the overall ability to classify even more. Using the classification coefficients generated by the discriminant analysis with the dependent data set, a number of spectral exposure measurements that were taken along with the original data were tested as an independent data set. Seventy six percent of the data set was correctly classified and it was shown that spectral information from four Landsat 2 spectral bands can in fact enable the classification of known and unknown geologic types.

Several major trends were shown in the project enabling the classification of a series of geologic groups from the space-born platform with an overall accuracy of 77.82 and 74 percent for the dependent and independent data set. A ratio mask of spectral bands 5 and 7 was made and it was shown that resulting reflectance ratios of the test

geologic groups, are measureably different. The use of digital images in the form of computer compatable tape would enable analysis that would be more objective and would give better representation of the physical phenomenon being investigated. This is suggested for future work.

REFERENCES

1. American Society Of Photogrammetry, MANUAL OF REMOTE SENSING, Falls Church, Va., 11, 1975, p5

2. Sigeal, Gilespie, REMOTE SENSING IN GEOLOGY, McGraw-Hill Books, 1980, p258

3. Lillesand, Kiefer, REMOTE SENSING AND IMAGE INTERPRETATION, New York, John Wiley & Sons, 1979, p 378

4. Elaison, Soderblom, Chavez "Extraction of Topographic and Albedo Information from Multispectral Images," PHOTOGRAMMETRIC ENGINEERING AND REMOTE SENSING, 46, 11, (1981), pp1571-1579

5. Bastion, Edwards, Elaison, "Synthetic Stereo and Landsat Pictures," PHOTOGRAMMETRIC ENGINEERING AND REMOTE SENSING, 42, 2, (1976)., pp 1279-1284

6. Dear, Spencer, "Evaluation of Photographic Enhancements of Lanosat Imagery," REMOTE SENSING OF ENVIRONMENT, 12, (1982), pp381-390

7. Piech, Walker, "Interpretation of Soils," PHOTOGRAMMETRIC ENGINEERING, 40, (1974), pp 87-94

8. IBID.

9. Lillesand and Kieffer, p 371

10. Piech and Walker, "Interpretation of Soils", pp 87-94

11. Piech, Walker, "Aerial Color Analysis of Water Quality," JOURNAL OF SURVEYING AND MAPPING DIVISION, ASCE, 97, No SU2, (1971), pp 185-197

12. Ibid.

13. Dr. J. Schott, Personal Communication, 1984

14. Smith, Piech, Walker, "Special Color Analysis Technique," PHOTOGRAMMETRIC ENGINEERING, 40, (1974), pp 1315-1322

15. Siegal, Gilespie, REMOTE SENSING IN GEOLOGY, McGraw-Hill Books, 1980, p258

16. Dr. E. Granger, Personal Communication, 12/15/84

17. United States Department of Commerce, National Oceanic and Atmospheric Administration, LANDSAT FACT SHEET, EROS Data Center, Sioux Falls, SD 57198

18. Dr. John Schott, Personal Communication, 1983

19. Dean and Spencer.

20. USGS, LANDSAT FACT SHEET., p6

21. Elvidson, Soderblom, Chavez, pp 1571-1579

22. IBID.

23. Holmes, Nueson, Vincent, "Optimum Thermal Infared Bands for Mapping General Rock Type and Temperature from Space," REMOTE SENSING OF ENVIRONMENT, 9, (1980), pp 247-263

24. Smith, Piech, Walker, pp 1315-1322

25. Dean and Spencer.

26. Dr. J. Schott, Personal Communication, 1984

27. N. Nie, C. Hull, J. Jenkins et al, STATISTICAL PACKAGE FOR THE SOCIAL SCIENCES, second ed, New York, McGraw-Hill Book Co, 1975, pp 434-467

28. Donald F. Morrison, MULTIVARIATE STATISTICAL METHODS, New York, McGraw-Hill Book Co. 1965, p 80

29. Anderson, T.W., AN INTRODUCTION TO MULTIVARIATE STATISTICAL ANALYSIS, John Wiley and Sons Inc, New York, 1958

30. Siegrist, Schnetzler, "Optimum Spectral Bands for Rock Discrimination," PHOTOGRAMMETRIC ENGINEERING AND REMOTE SENSING, 46, 9, (1980), pp 1207-1215

31. Douglas C. Montgomery, DESIGN AND ANALYSIS OF EXPERIMENTS, New York, John Wiley & Sons, 1976, p 34

32. Davis, Landgrebe, et al, REMOTE SENSING, THE QUANTITATIVE APPROACH, New York, McGraw-Hill Books, 1978, p36

33. IBID, p 35

34. Don Marsh, Lab Notebook, Fall Quarter 1984

35. UTAH GEOLOGICAL AND MINERAL SURVEY Map, compiled by Leni F. Heintz, 1980, scale = 1:500,000

36. United States Geological Survey Maps, I-377 (1963), I-378 (1963), GQ-154 (1962), GQ-155 (1961)

37 Irwin Miller and John E. Freund, PROBABILITY AND STATISTICS FOR ENGINEERS, Englewood Cliffs, New Jersy, Prentice-Hall Inc., p174

APPENDIX

Appendix 1.

Scale Calculation

$$\text{Photo Scale} = \frac{\text{photographic distance}}{\text{ground distance}}$$

Appendix 2.

Basis For Contrast Calculation Program [courtesy Dr. J. Schott]

Given $D = -\gamma \text{Log } E + K$

1, - indicates pos. film

2 - assumption of linearity inherent in expression

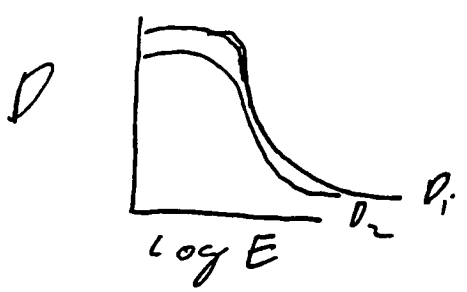

Figure 1

D_2 is the contrast reduced curve due to flare. If we plot density versus $(E - \beta) = \gamma R$ for original film

D_3 is some high contrast curve which would offset the flatening effects of β such that the original curve D_1 would be a plot of E vs γ R

How might we go about this

$$D_1 = -\gamma_1 \text{ Log } E_1 + k_1$$

on processing a step wedge in a Black and White processor

$$D_p = \gamma_p \text{ Log } E_p + k_p$$

where γ_p is a function of film type
chemistry type
chem. concentration
time in developer
temperature of developer

For a contact separation

$$F = I \cdot T_F \cdot T_{FILM} = I\, T_F \cdot 10^{-D_{FILM}}$$

where I is intensity of the source of the film
T_F is transmission of the film
T_{FILM} is transmission of the film

$$D_{p1} = \gamma_p \text{ Log } IT_F\, 10^{-D_1} + k_p$$

NB - assumption of linearity is very good because we can choose the position on the curve

$$= \gamma_p \text{ Log } [-(-\gamma_1 \text{ Log } E_1 + k_1)] + k_p + \gamma_p \text{ Log } IT_p$$

$$= \gamma_p \gamma_1 \text{ Log } E_1 + \gamma_p k_1 + k_p + \gamma_p \text{ Log } IT_p$$

$$D_{p1} = \gamma_p \gamma_1 \text{ Log } E + k_2$$

$$D_{p1} = \gamma_1 \text{ Log } E^{\gamma_p} + k_2$$

How can we utilize this control over γ to enhance the contrast and obtain a linear relationship between density and reflectance

(at the time controls on density slicing devices didn't exist)

(still valuable due to increased γ)

$$D = -\gamma_1 \text{ Log } E + k_1 \quad \gamma = \gamma_1 \text{ Log } (R) + k_2$$

$$\gamma = \gamma_p$$

On separation and processing

$$D = \gamma_1 \text{ Log } E^{\varepsilon} + K_E \quad \gamma = \gamma_1 \text{ Log } (R) + k_2$$

On density slice were concerned about ΔD values

$$D_1 - D_2 = \Delta D = \gamma_1 \text{ Log} \left(\frac{E_1}{E_2}\right)^{\varepsilon} \simeq \gamma_1 \text{ Log } \frac{R_1}{R_2}$$

For this to be true

$$\left(\frac{E_1}{E_2}\right)^{\varepsilon} = \frac{R_1}{R_2}$$

or we can choose ε such that

$$\left(\frac{E_1}{E_2}\right)^{\varepsilon} - \frac{R_1}{R_2} \quad \text{be a minimum} \qquad (1)$$

where the remainder is a measure of the error term.

We want the above to be true for values of $\frac{E_1}{E_2}$ from $\frac{E_{min}}{E_{max}}$ to $\frac{E_{max}}{E_{min}}$

can run on iterative program to find ε .

Can we write a more general expression so we don't need to do the computation each time?

Let X1 $\cdot\beta$ Be exposure = E_1 at Pt. 1

X2 $\cdot\beta$ Be exposure = E_2 at Pt. 2

Then (X1-1)β is the R_1 ~~V = E_{V2} at 1~~ value at point 1

(X2-1)β is the R_2 ~~V = E_{V2} at 2~~ value at point 2

Inserting in 1.

$$\left(\frac{X1}{X2}\right)^{\varepsilon} - \frac{X1-1}{X2-2}$$ Be a minimum

For range of $\frac{X1}{X2}$ from values of interest

*There are limits however on [illegible] ~~5 = 2 = 5~~

Equivalent to

$$\left(\frac{E_1}{E_2}\right)^{\varepsilon} - \frac{R_1}{R_2}$$ Be a minimum

Then on slicing

$D \approx \text{Log } R + k$ with predictable error terms

The expression above could be tabulated for rapid access from inputs of a range of exposure values of interest expressed as multiples of P .

For Mask:

$X1 \cdot \beta_x = E_1$ for Bard x

$X2 \cdot \beta_x = E_2$ for Bard x

$(X1 - 1)_x$
$(X2 - 1)_x$ corresponding ΔR values

$Y1 \cdot \beta_y$ $(X1 - 1) \cdot \beta_y$
$Y2 \cdot \beta_y$ $(Y2 - 2) \cdot \beta_y$ corresponding values for Bard Y

$$D_y = -\gamma_y \text{ Log } E_y + k$$

Process

$$D_y = \gamma_y \text{ Log } E_y^{\xi_y} + k$$

Unit reverse process

$$D_y = -\gamma_y \text{ 10g } E_y^{\xi_y} + k = -\text{ Log } E_y^{\xi_y \gamma_y}$$

Process reverse x

$$D_x = \gamma_x \text{ Log } E_x^{\xi_x} + k = \text{Log } E_x^{\xi_x \gamma_x}$$

Sandwich

$$D_M = D_x + D_y = \text{Log } \frac{E_x^{\xi_x \gamma_x}}{E_y^{\xi_y \gamma_y}} + k$$

$$\Delta D_M = \text{Log} \frac{E_{x1}^{\varepsilon_x \gamma_x}}{E_{y1}^{\varepsilon_y \gamma_y}} - \text{Log} \frac{E_{x2}^{\varepsilon_x \gamma_x}}{E_{y2}^{\varepsilon_x \gamma_y}}$$

$$= \text{Log} \frac{E_{x1}^{\varepsilon_x \gamma_x}}{E_{y1}^{\varepsilon_y \gamma_y}} \cdot \frac{E_{y2}^{\varepsilon_y \gamma_y}}{E_{x2}^{\varepsilon_x \gamma_x}}$$

Substituting

$$\Delta D_M - \underbrace{\text{Log} \frac{X1^{\varepsilon_x \gamma_x}}{Y1^{\varepsilon_y \gamma_y}} \cdot \frac{Y2^{\varepsilon_y \gamma_y}}{X2^{\varepsilon_x \gamma_x}}}_{U} \approx \gamma_x \underbrace{\text{Log} \frac{(X1-1)\ (Y2-1)}{(X2-1)\ (X2-1)}}_{V}$$

So choose ε_x by the method for single layer;then choose ε_y such that

Log u - γ_x Log V be a minimum for all interested values of E_x and E_y expressed as multiples of ε_x and ε_y .

ε_y can be calculated as follows:

$$D_y = \gamma_y \text{Log} \frac{E_1^{\varepsilon_y}}{E_2} = \gamma_x \text{Log} \frac{R_1}{R_2}$$

and know from single variable or $\frac{\gamma_y \varepsilon_y}{\gamma_x} \text{Log} \frac{E_1}{E_2} = \text{Log} \frac{R_1}{R_2}$

$$D = \gamma_1 \text{Log} \left(\frac{E_1}{E_2}\right)^{\varepsilon_1} = \gamma_1 \text{Log} \frac{R_1}{R_2}$$

or $\varepsilon_1 \text{Log} \frac{E_1}{E_2} = \text{Log} \frac{k_1}{k_2}$

So $\varepsilon_y \frac{\varepsilon_y}{\varepsilon_x} = \varepsilon_1$

$$\varepsilon_y = \varepsilon_1 \frac{2}{y}$$

where ε_1 is calculated for Y range and single layer case

Since

$$D_x = \gamma_x^1 \text{ Log } R_x + k$$

$$D_y \cong - \gamma_x^1 \text{ Log } R_y + k$$

$$\Delta D = \gamma_x^1 \text{ Log } \frac{R_x}{R_y} + k$$

i.e., D mask is linear with the R ratio if R_y and D_y are chosen linear in the same manner.

The error terms are higher in that process because they are minimized separately and then combined rather than minimizing the combination.

Neglecting linearity, i.e.

Let $D_1 = \gamma_1 (\text{Log } E)^3 + \gamma_2 (\text{Log } E)^2 + Y_3 \text{ Log } E + k$
or higher order terms

$D_p = \gamma_{p1} (\text{Log } E_p)^3$

$E_p = 10^{-D_1} \; T_{\text{Filters}} \; I_{\text{Source}}$

etc.

The math look nasty but the process is straightforward and requires only some mathematic manipulations, etc. and if desired much of the middle can be omitted. It is merely necessary to analyze what the relationship between D mask and $\frac{R_x}{R_y}$ is and slice the image accordingly.

More detail is required only if the nature of the relationship is to be predetermined such that is enhanced and errors minimized over certain areas.

Figure 2 displays a single variable error plot. Interpretation is such that when curve is flat over range of E values, choose value of that curve. As E 1B it becomes more and more difficult to have linear relationship, i.e., error terms increase.

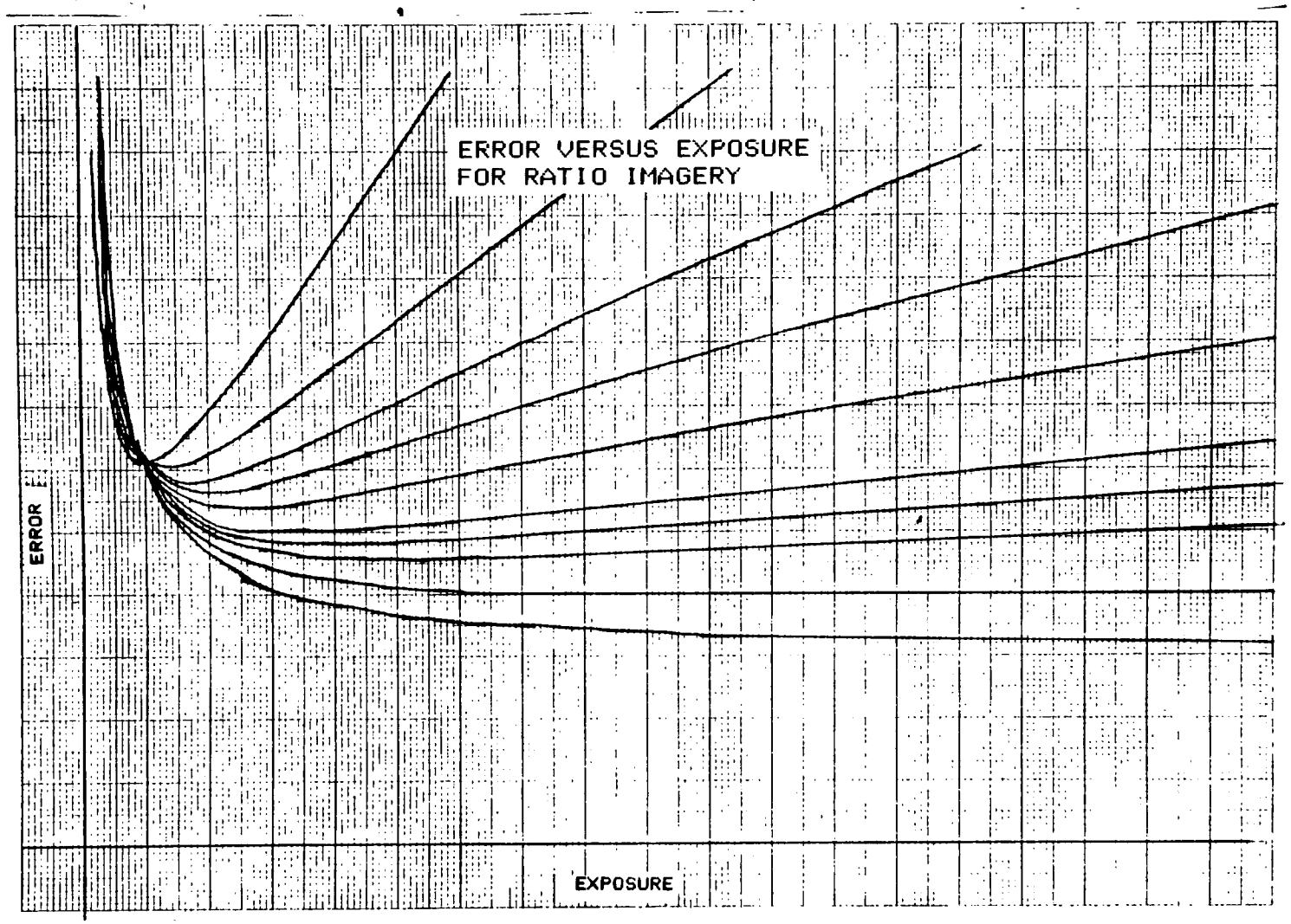
ERROR VERSUS EXPOSURE
FOR RATIO IMAGERY
ERROR
EXPOSURE

Appendix B.

Calculation of Coefficients:

$$r_{ij} = \frac{\mathrm{cov}(X_i, X_j)}{\mathrm{sqrt}\left[\ \mathrm{var}(X_i)\ \mathrm{var}(X_j)\ \right]}$$

In the matrix form:

$$R = \begin{bmatrix} 1 & \rho_{12} & \cdots & \rho_{1\eta} \\ \rho_{12} & 1 & \cdots & \rho_{2\eta} \\ \cdots & \cdots & \cdots & \cdots \\ \rho_{1\eta} & \rho_{2\eta} & \cdots & 1 \end{bmatrix}$$

Appendix A.

SPSS Command File.

```
RUN NAME          THESIS SYNTHETIC DATA RATIO-SET ANALYSIS
INPUT MEDIUM      CARD
N OF CASES        4
VARIABLE LIST     CASE.ID,EX1,EX2,EX3,EX4,EX5/
INPUT FORMAT      FREEFIELD
DISCRIMINANT      GROUPS = CASE (1,4)/VARIABLES = EX1,EX2,EX3,EX4,EX5,CASE
                  ANALYSIS = CASE /METHOD = WILKS/
OPTIONS           13,5,6,7,8,11,12,17,18,19
READ INPUT DATA
11 229.1 229.1 195.0 251.2 275.4
12 218.8 158.5 73.8  154.9 208.4
13 933.3 1202  851.1 1071  1122
14 64.57 61.66 70.79 75.86 75.86
15 36.31 36.31 38.90 38.90 40.74
16 93.33 134.0 125.9 125.9 144.5
17 8.510 6.310 10.00 7.940 7.940
21 97.72 114.8 109.7 109.2 97.72
22 63.10 72.44 41.69 44.67 63.10
23 831.8 891.3 1000  1000  977.2
24 214.5 15.85 15.49 15.85 13.49
25 12.30 9.12  11.48 13.18 12.30
26 19.95 23.44 23.44 21.88 21.88
27 2.240 2.750 3.160 2.510 2.240
31 102.3 147.9 138.0 114.8 147.9
32 17.38 14.45 14.45 18.62 13.18
33 1995  2754  2188  2188  1698
34 21.38 22.39 22.91 26.92 26.92
35 17.38 17.38 15.85 18.62 15.85
36 29.02 25.70 44.67 31.62 28.02
37 5.010 3.390 2.510 2.510 3.160
41 51.29 45.71 31 29 51.29 45.71
42 17.95 26.92 14.45 20.41 23.84
43 794.3 660.7 741.3 794.3 707.9
44 2.040 2.510 2.820 2.690 3.160
45 5.010 6.760 8.320 6.310 6.460
46 9.950 9.950 14.13 19.95 12.50
47 2.690 2.690 4.070 2.340 3.160
FINISH
```

Appendix 5. Equipment and Supplies.

- "Big" Roscoe Microdensitometer. Gratis PPHS @ R.I.T.
- McBeth RD-100 Reflection Densitometer
- Landsat 2 Multispectral Scene 21685-17255
- United Geological Survey Maps .....
- Test rock types supplied, Misco Biological Inc. rock se #52e20

including the following rock types:

1. Phyllite	2. Garnet Schist
3. Quartzite	4. Red Slate
5. Grey Slate	6. White Marble
7. Graphite	

- Kodak wratten filters, #2, #3, #4 and glass filter 3014.
- Kodak High Speed Infared Film 2481 (ESTAR Base) [used for test imagery]
- Kodak Fine Grain Positive Film 7302 [used for production of ratio image]
- Kodak Versamat Film Processor, Model 5
- VAX 11780 Computer System, SPIS software

```
]LIST

2  DIM ARR(2): DIM ADD(2)
5  GOTO 25
10  REM  THIS PROGRAM IS MADE
                        FOR THE THES
     IS RESEARCH
     PROJECT OF D.J.MARSH
                    MADE DURING THE
     QUARTER                    832
15  REM  THE FOLLOWING PROGRAM
                        WILL SOLVE A
      SET OF
     ANALYTICAL EQUATIONS FOR
                    MASK CONTRAST VA
     LUES FOR
18  REM  THE PROJECT "PHOTOMETRIC
                        PROCESSING A
     ND INTERPRETATION
     OF RATIOED IMAGERY FOR
                    SEPARATION OF GR
     OUND FEATURES.
20  REM  **********************
25  HOME
30  VTAB 10: HTAB 5
35  INVERSE : FLASH : PRINT "WELC
     OME TO THESIS PROGRAM 1"
37  VTAB 11: HTAB 10
40  PRINT "BY DON MARSH."
45  NORMAL
50  FOR I = 1 TO 1000
51  NEXT I
80  GOSUB 1000
85  PRINT "PLEASE INPUT THE TWO S
     PECTRAL BANDS ": PRINT "BEIN
     G USED."
90  INPUT A1,A2
95  GOSUB 1000: PRINT "WHICH SPEC
     TRAL BAND WILL BE COPIED": PRINT
     " EXACTLY WITH THE INVERSE S
     IGN CONTRAST?"
97  INPUT RR
```

```
100  GOSUB 1000: PRINT "INPUT THE
      CONTRAST VALUE OF SPECTRAL
     ": PRINT " BAND"RR
105  INPUT Z1
120  GOSUB 1000: PRINT "PLEASE IN
     PUT MAXIMUM AND MINIMUM": PRINT
     " EXPOSURE VALUES FOR BAND":
      PRINT A1
125  INPUT X1,X2
130  GOSUB 1000: PRINT "INPUT MAX
     IMUM AND MINIMUM EXPOSURE": PRINT
     " VALUES FOR BAND ": PRINT A
     2
135  INPUT Y1,Y2
190  GOTO 300
200  REM
300  REM
310 A = X1 / X2
320 B = Y1 / Y2
330 C = X2 / X1
340 D = (X1 - 1) / (X2 - 1)
350 E = (Y1 - 1) / (Y2 - 1)
360 F = Y2 / Y1
370  PRINT "**********************
     ********"
372  PRINT "*** OUTPUT CONTRAST V
     ALUES ***"
374  PRINT "**********************
     **********"
400  FOR E2 = (Z1 - 0.5) TO (Z1 +
     0.5) STEP 0.05
410 E1 = (0.4342945 *  LOG (C)) +
     (0.4342945 *  LOG ( ABS ((D +
     E) - (10 ^ E2) * F)))
425  PRINT "ORIGIONAL       COPY"
426  PRINT " CONTRAST      CONTRAS
     T"
430  PRINT E2,E1
440  NEXT E2
999  GOTO 1001
1000  HOME : VTAB 18: RETURN
1001  END
```

Appendix 7. Annotation of Test Sites and Names

Number	Site	Name
1	1 & 15	Lake Bonniville Deposits
2	2 & 9	Miocene Volcanic Rocks
3	3 & 16	Oligocene Volcanic Rock
4	4 & 5	Balsalt and Rhyolite
5	6	Older Alluvial Deposits
6	7	McCoy Creek & Sheprock Groups
7	8	Temple Butte Formations
8	10	Landslides
9	11	Navajoe Sandstone
10	12	Prospect Mountain Quartzite
11	13	White Sage Formations
12	14	Alluvium and Colluvium
13	17	Balsalts
14	18	Cretaceous Formations
15	19	Arapian Shale

VITA

Don is a fourth year student at the Rochester Institute of Technology seeking a Bachelors degree in Imaging and Photographic Science. Don has lived in the Rochester area for most of his life and became interested in photography his 9th grade of high school. Pursuing his interest in science and photography, Don started his college career in 1980 at R.I.T. and became a member of several photographic interest groups. Continuing an interest in remote sensing and digital image processing, Don hopes to complete a Masters degree in this discipline in the near future.